Supporting Information

Study of oxygen vacancies in TiO_2 nanostructures and their relationship with photocatalytic activity

Alba Arenas-Hernandez[1*], Carlos Zuñiga Islas[1], Mario Moreno[1], Wilfrido Calleja Arriaga[1], Julio César Mendoza-Cervantes[1], Netzahualcoyotl Carlos[1], Carlos Roberto Ascencio-Hurtado[1], Aurelio Heredia Jiménez[2]

[1]National Institute of Astrophysics, Optics and Electronics (INAOE); Electronics, Tonantzintla, Puebla, Mexico.
[2] Popular Autonomous University of the Puebla of State (UPAEP); Electronics, Puebla, Puebla, Mexico.
***Corresponding authors: E-mail: alba.arenas@inaoep.mx and albaarenas.inaoep@gmail.com**

This section was elaborated to support the results of manuscript, here many experiments were included like EDS, dye degradation using a UV lamp without catalyst, degradation using scavengers and TRPL study.

1.- The elemental chemical composition of TiO_2 nanostructures on titanium foil are shown in Table S1. As can be noticed, chemical elements such as N and F were detected, which correspond to the organic electrolyte solution [1]. The relationship between O and Ti is closed to stoichiometry for TiO_2-nt. Whereas self-assembled nanostructures had a lower oxygen content, which may be related to defect states, specifically oxygen vacancies due to deficiency of oxygen in the TiO_2 film [2, 3]. According to D. Acharyya et al., the non-stoichiometry of metal oxides can be caused by titanium interstitials and oxygen vacancies [3-5].

Table S1. Summary of elemental composition of TiO_2 nanostructures.

Nanostructure	N At%	O At%	F At%	Ti At%
TiO_2-nt	5.92	58.72	1.13	31.62
TiO_2-nc	7.1	42.76	9.29	34.3
TiO_2-ns/TiO_2-nc	7.19	45.69	6.65	34.19
TiO_2-nb/TiO_2-nc	5.69	42.13	7.93	41.99

2.- XRD patterns of TiO_2 nanostructures are illustrated in Figure S1. The Ti peaks were localized at 25°, 48°, 54°, 55°, and 62.8° corresponding to the planes (101), (200), (105), (211), and (204), respectively. Moreover, the planes of anatase phase (101), (004), (200), (105), (002), (220), (215) and (301) were localized at 25.25°, 37.92°, 48.02°, 54.55°, 62.71°, 70.30°,75°, 76.02°, respectively [2, 6-8]. A significant intensity of plane (101) was observed for nanotubes, which had the highest intensity. In contrast, the TiO_2-nb/TiO_2-nc had a lower intensity than other TiO_2 films. From Raman characterization, an effect of thickness on intensity can be observed. Therefore, the XRD results confirms the thickness effect on structural

properties. Other important plane of nanostructures is the plane (002), which had a similar intensity for the four films.

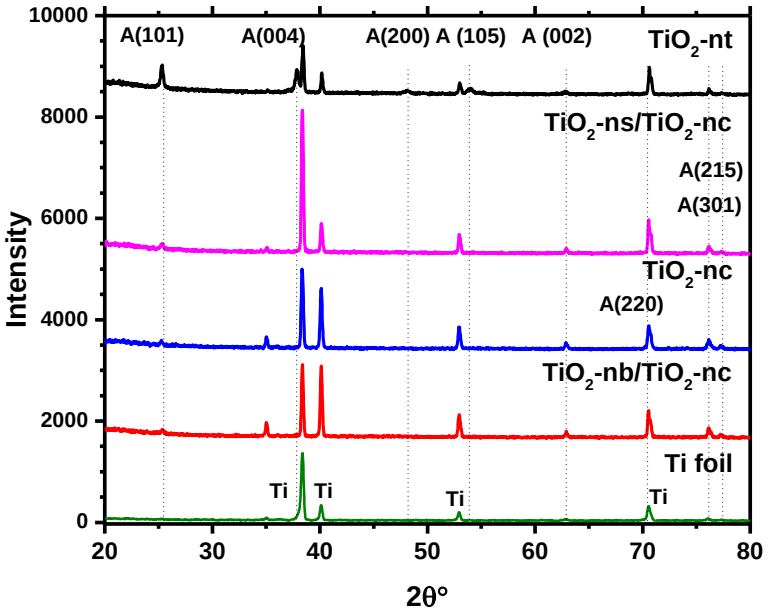

Figure S1. Summary of elemental composition of TiO_2 nanostructures.

3.- The scavenging experiments were carried out to analyze the active species on TiO_2-ns/TiO_2-nc. According to Nobuaki Shimizu et al. methanol is used as the scavenger of h^+, whereas 2-propanol is used for OH^-. Superoxide dismutase was used as scavenger for superoxide radical anions [9-11]. As can be observed in Figure S2, the degradation of methylene blue decreased with h^+ scavenger to 33.6%. When the OH^- scavenger is used, the degradation also decreases (52.8%). A lower degradation was observed using $O_2^{\cdot -}$ scavenger of 31.21%. Therefore, the key active specie for TiO_2-ns/TiO_2-nc is $O_2^{\cdot -}$. Due to the elimination of $O_2^{\cdot -}$, the degradation was decreased.
These results help to understand the importance of oxygen vacancies in TiO_2 film.
As is known, oxygen vacancies are electron donor sites, when O_2 is absorbed by oxygen vacancies, it reacts with electrons to form superoxide radicals.
Oxygen vacancies in combination with holes and hydroxyl radicals promote reduction and oxidation processes for catalytic performance [9-11].

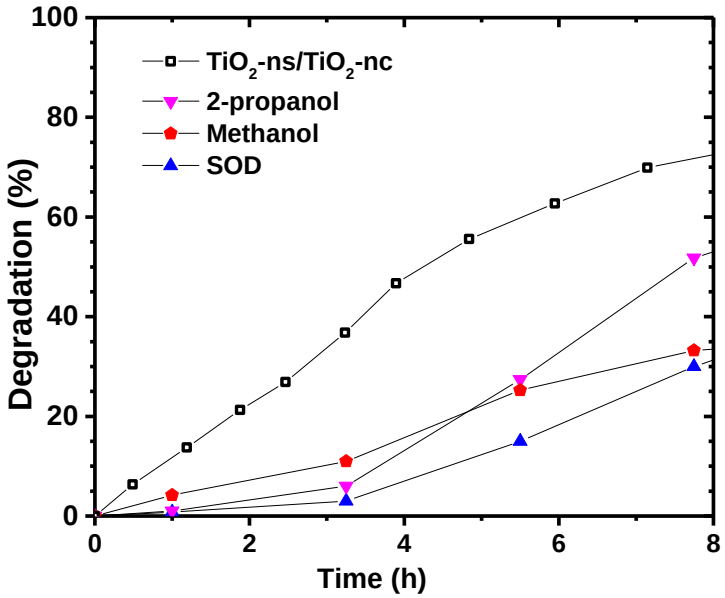

Figure S2. Photodegradation of methylene blue using TiO_2-ns/TiO_2-nc, and scavenging experiments.

4.- In order to understand the effect of oxygen vacancies on catalysis, the TRPL spectra are illustrated in Figure S3. Here, the TRPL spectra were calculated at 418 nm, 448 nm, and 532 nm, which correspond to STE, Vo*, and Vo**, respectively. The lifetime was determined by a three-exponential decay function and t_{av} (ns) was calculated according to equation of the reference [14-15]. According to PL results, the sample studied here has the highest number of Vo*.

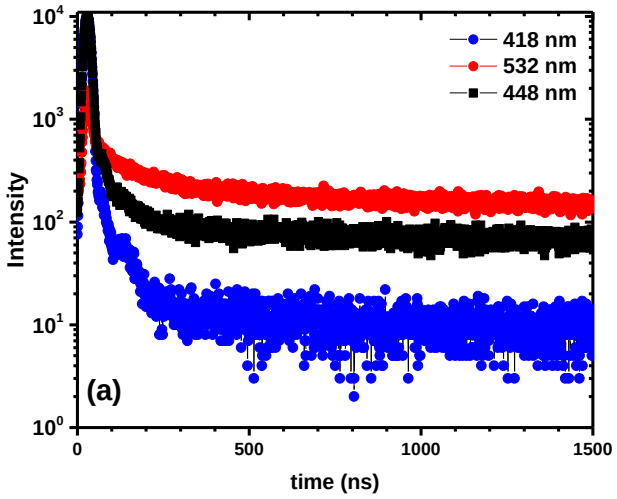

Figure S3. TRPL spectra of TiO_2 nanomaterial with higher number of oxygen vacancies.

As it can be seen, in Table S2, the lifetime of carriers increases significantly at 448 nm, which is related to single-ionized oxygen vacancies. Also, the lifetime of carriers increases with peak correspondently to doubly-ionized oxygen vacancies. To validate the effect of concentration of oxygen vacancies in Table S2, is shown the lifetime of TiO_2 nanomaterial with the lower amount of single-ionized oxygen vacancies (peak at 448 nm*). Therefore, the amount of oxygen vacancies increases the lifetime of photogenerated carriers, and this affects the catalysis process because more active species participate in the reduction and oxidation processes [8, 14, 15]. These results are similar to other reports where determined the effect of oxygen vacancies on catalytic activity [14-17].

Table S2. Lifetime of photogenerated carriers of TiO_2 materials.

	t_1 (ns)	t_2 (ns)	t_3 (ns)	t_{av} (ns)
418 nm	3.74	3.74	52.68	27.71
448 nm	2.78	38.06	358.95	55.21
532 nm	3.96	61.32	310.29	215.48
448 nm*	35.88	2.41	250	64.25

References

1.-Arenas-Hernandez A.; Zúñiga-Islas C.; Mendoza-Cervantes J. C. A study of the effect of morphology on the optical and electrical properties of TiO_2 nanotubes for gas sensing applications. Eur. Phys. J. Appl. Phys. 2020, 90, 30102

2.-Verma R.; Samdarshi S.K. Correlating oxygen vacancies and phase ratio/interface with efficient photocatalytic activity in mixed phase TiO_2. Journal of Alloys and Compounds. 2015, 629, 105

3.- Acharyya D., Hazra A., Bhattacharyya P. A journey towards reliability improvement of TiO_2 based Resistive Random Access Memory: A review. Microelectronics Reliability. 2014, 54, 3, 541-560

4.- Sarkar Ayan; Gopa Khan Gobinda. The Formation and Detection Techniques of Oxygen Vacancies in Titanium Oxide-based Nano-structures. Nanoscale 2019, 11, 3414

5.- Lin Niu; Xiaoli Zhao; Zhi Tang; Hongzhou Lv; Fengchang Wu; Xiaolei Wang; Tianhui Zhao; Junyu Wang; Aiming Wu; John. P. Giesy. Difference in performance and mechanism for methylene blue when TiO_2 nanoparticles are converted to nanotube. Journal of Cleaner Production. 2021, 297, 126498

6.-Hongchao Li; Ningxin Tang; Hongzhi Yang; Xian Leng; Jianpeng Zou. Interface feature characterization and Schottky interfacial layer confirmation of TiO_2 nanotube array film. Applied Surface Science. 2015, 355, 849–860

7.- Yulong Liao; Botao Yuan; Dainan Zhang; Xiaoyi Wang; Yuanxun Li; Qiye Wen; Huaiwu Zhang; and Zhiyong Zhong; Liao et al. A Facile Method for Loading CeO2

Nanoparticles on Anodic TiO_2 Nanotube Arrays. Nanoscale Research Letters. 2018, 13, 89

8.- Biswajit Choudhury; Sayan Bayan; Amarjyoti Choudhury; Purushottam Chakraborty. Narrowing of band gap and effective charge carrier separation in oxygen deficient TiO_2 nanotubes with improved visible light photocatalytic activity, Journal of Colloid and Interface Science. 2016, 4651–10

9.- Nobuaki Shimizu; Chiaki Ogino; Mahmoud Farshbaf Dadjour; Tomoyuki Murata. Sonocatalytic degradation of methylene blue with TiO_2 pellets in water Ultrasonics Sonochemistry. 2007, 14,184–190

10.- Etacheri V.; Di Valentin C.; Schneider J.; Bahnemann D.; Pillai S.C. Visible-Light Activation of TiO_2 Photocatalysts: Advances in Theory and Experiments. Journal of Photochemistry and Photobiology C:Photochemistry Reviews. 2015, 25, 1-29

11.- Xinggang Hou; Xiaoli Liu; Jing Han; Huanli Liu; Jianghong Yao; Dejun Li; Liqun Wang; Bin Liao; Jing Li; and Ruijing Zhang. Enhanced photoelectrocatalytic degradation of organic pollutants using TiO_2 nanotubes implanted with nitrogen ions. Journal of Materials Science. 2020, 55, 14, 1-18

12.- Yi-Hsuan Chiu; Tso-Fu Mark Chang; Chun-Yi Chen; Masato Sone; Yung-Jung Hsu. Mechanistic Insights into Photodegradation of Organic Dyes Using Heterostructure Photocatalysts. Catalysts. 2019, 9, 430

13.- Pei Zheng; Zhe Pan; Hongying Li; Bo Bai; Weisheng Guan. Effect of different type of scavengers on the photocatalytic removal of copper and cyanide in the presence of TiO_2@yeast hybrids. Journal of Materials Science: Materials in Electronics. 2015, 26, 9

14.- Ying-Chih Pu; Hsin-Ying Chou; Wen-Shuo Kuo; Kung-Hwa Wei; Yung-Jung Hsu. Interfacial charge carrier dynamics of cuprous oxide-reduced graphene oxide (Cu2O-rGO) nanoheterostructures and their related visible-light-driven photocatalysis. Applied Catalysis B, Environmental. 2017, 204, 21-32

15.- Qi Wanga; Shan Zhanga; Hanna Heb; Chunlin Xiea; Yougen Tanga; Chuanxin Hee; Minhua Shao; Haiyan Wanga. Oxygen Vacancy Engineering in Titanium Dioxide for Sodium Storage, Chem. Asian J. 2021 16, 1, 3

16.- Yi-Fang Lin; Yung-Jung Hsu. Interfacial charge carrier dynamics of type-II semiconductor nanoheterostructures. Applied Catalysis B: Environmental. 2013, 130–131, 93–98

17.- Wu S; Tan X; Liu K; Lei J; Wang L; Zhang J. TiO_2 (B) nanotubes with ultrathin shell for highly efficient photocatalytic fixation of nitrogen. Catalysis Today. 2018, 335, 241-220